

INVESTIGATION OF CLOUD PROPERTIES AND ATMOSPHERIC STABILITY WITH MODIS

SEMI-ANNUAL REPORT FOR JUL-DEC 1995

Paul Menzel

NOAA/NESDIS at the University of Wisconsin

Contract NAS5-31367

ABSTRACT

In the past six months, all beta software were delivered, the spectral and radiometric performance of the MAS (MODIS Airborne Simulator) were characterized, and the SCAR-B field experiment was supported daily with real time analysis of the biomass burning and associated smoke in South America. In addition, UW hosted a MODIS cloud mask meeting and the MCST thermal calibration audit.

TASK OBJECTIVES

Software Development

Work continues on evolving the three software packages (cloud mask, cloud top properties, and atmospheric profiles) from AVHRR, HIRS, and MAS data to MODIS data. Beta 3 software were delivered to the SDST by the end of October 1995. MODIS cloud mask data sets in different land/ocean and winter/summer regimes were developed with AVHRR and MAS data; feedback from the MODIS community is now being solicited. High resolution cloud masks using MAS 50 channel data of different atmospheric and surface regimes (a Gulf of Mexico tropical data set (January 1995) and an Alaskan polar data set (April 1995)) were also processed using an updated algorithm within the last quarter and will be distributed next quarter.

Evolving the ATBDs

The UW ATBDs will be revised to include information from the continuing MAS, AVHRR, HIRS, and GOES cloud investigations. Another version of the ATBDs will be drafted in early 1996.

Algorithm Definition

Processing and testing of the cloud parameter algorithms (mask, temperature, phase, height, and amount) will continue using the MAS data at UW. Algorithms for atmospheric total column amount (ozone, precipitable water vapor, and stability) and profiles (temperature and moisture) will be developed using the GOES-8 and HIRS data from the field experiment completed with the MAS and HIS in January 1995.

UW will support the SASS field experiment in April 1996 to gather more measurements of thin cirrus and aircraft contrails.

Global Cloud Study

Pre-MODIS cloud studies will continue via the global cloud census with HIRS data now in its seventh year.

MODIS Infrared Calibration

Postlaunch procedures for validating MODIS radiances will continue to be refined; an initial demonstration using GOES-8 with underflights of the MAS and HIS in January 1995 was successful. Prelaunch calibration of the MODIS infrared channels requires considerable testing to characterize detector to detector and band to band cross talk, detector non-linear response, stray radiation, scan mirror emissivity variations with angle and wavelength, angle dependence of background radiation, and other effects. The Engineering Model thermal vacuum tests are being studied to reveal answers and questions; Flight Model test data will be investigated to see how far we have progressed..

WORK ACCOMPLISHED

MODIS Software Development and Deliveries

Considerable effort was spent in preparation for the MODIS Beta software deliveries, culminating in updated Beta 3 deliveries of the cloud mask, cloud top properties, cloud phase and atmospheric profiles production software. Beta software development involved several steps:

(1) Hal Woolf computed MODIS IR band transmittance profiles with a new regression-based band transmittance model, using the MODIS specification spectral response data delivered by SDST in September 94. The model was developed using a 32 atmosphere dependent set, and FASCODE transmittance profile computations at 6 equally spaced sensor zenith angles from nadir to 63.5 degrees. This method has been used for other sensors including HIRS, GOES, and AVHRR. A profile of transmittances at 40 standard pressure levels from 0.1 (space) to 1000 mb was derived.

(2) Chris Moeller wrote code to convert simulated MODIS IR band radiance ($\text{W}/\text{m}^2/\text{ster}/\mu\text{m}$) to brightness temperature (K), and then to UW-preferred radiance units ($\text{mW}/\text{m}^2/\text{ster}/\text{cm}^{-1}$) over the temperature range 180 to 320K.

(3) Liam Gumley generated software to read the simulated MODIS Level-1B and geolocation data sets required to use the data with the current UW MODIS algorithms. SDST simulated MODIS Level-1B data were received in September 1995 and Rich

Hucek of the MODIS SDST provided important assistance for interpreting the simulated data. All of the UW MODIS algorithms are now able to read and process the MODIS simulated scan cubes. However it should be noted that there is little scientific value in the simulated data for our cloud and atmospheric profile products, since no clouds are included and clear-sky radiances appear to be suspect. UW will continue to use their MODIS-like simulated data (created from MAS, HIRS, and AVHRR) for testing and developing MODIS algorithms.

(4) UW MODIS algorithms can now use the PGS and MODIS API toolkits. Beta 3 delivery uses the toolkits for opening and closing files, accessing MODIS data, and message logging.

(5) MODIS product files were created using the Interface Control Documents (ICDs) as a guide. As far as possible UW duplicated the structure of the MODIS products outlined in the ICDs.

(6) Cloud top properties and atmospheric profiles MODIS production software are heavily based on heritage code; which doesn't conform to EOS production software standards. As a result, a considerable effort was made to update the code to meet EOS and MODIS software standards.

(7) Although the simulated radiances were of a clear atmosphere only, the cloud mask results were not high confidence clear for all pixels. Two main reasons for the lower confidence clear scenes were identified: (a) .87 micron channel reflectances were higher over water than .66 micron reflectances, an unrealistic occurrence. This led the reflectance ratio test to flag many of the water scenes as low confidence clear. The SDST has identified the problem in their simulation. (b) A 4 km land/sea mask was used in the simulated radiance generation, whereas the cloud mask uses a 1 km land/sea mask to determine the correct processing path. The resolution difference resulted in lower confidence clear values along land/water boundaries.

(8) After thorough testing, all beta delivery software were transferred to the SDST and accepted after successful check out.

Ancillary Data For MODIS Level-2 Processing

At the MODIS Science Interest Group Meeting in November 1995, SDST indicated that MODIS algorithm developers would be responsible for supplying ancillary datasets and necessary software tools for the Version 1 delivery in the first quarter of 1996. This prompted UW to investigate availability of gridded ancillary data. Real-time gridded analysis and forecast products are available via anonymous FTP from NMC, and several sample datasets in GRIB format were downloaded. FORTRAN code to unpack the GRIB data files was also obtained from NMC, and installed on the UW SCF. Using this software, it was possible to unpack all fields from an NMC 1x1 degree global gridded analysis data set, and to view the individual fields as images in

IDL. It appears that the data files found at NMC contain all the ancillary data items UW requires for Version 1, except for total ozone. However global gridded total ozone fields derived from HIRS are available in GRIB format from an anonymous FTP site at GSFC. Using the NMC software the data were unpacked and displayed as an image in IDL.

Creation of Simulated MODIS Level-1B Data Using MAS

Preliminary work was begun on creating a 36 channel simulated MODIS Level-1B data set using MAS data. UW plans to resample MAS 50 m pixels to 100 m and 200 m pixels in the same way that MODIS 250 m pixels map to MODIS 500 m and 1000 m pixels. Of the 50 MAS spectral bands, 19 are a close match with MODIS spectral bands. For the other 17 MODIS bands, UW will use information from MAS bands with similar spectral features where possible, and apply forward calculations elsewhere. Level-1B and geolocation files will be produced in HDF containing exactly the same parameters as the MODIS Level-1B simulated datasets produced at GSFC for the MODIS software Beta delivery in October 1995.

Cloud Mask Test Data Set Delivery

A global 1-day cloud mask data set has been created using AVHRR (Advanced Very High Resolution Radiometer) GAC (Global Area Coverage) radiances and delivered to the SDST for distribution. The data set was produced for the purpose of identifying problems associated with building the global MODIS cloud mask algorithm. A robust method must readily adjust to variations in illumination, surface properties, ecosystems, and atmospheric temperature and humidity structure. This effort is only preliminary in this respect.

The cloud mask algorithm utilizes visible and infrared spectral tests as well as spatial uniformity information and is divided into 7 conceptual domains; daytime land surface, daytime water, nighttime land, nighttime water, desert (daytime only), and daytime and nighttime polar regions. Ancillary data sets include the 10-minute Olson World Ecosystems and USGS 1 km land/sea tag files. No attention has been given to the nighttime desert and polar regions to date. Currently, the nighttime land algorithm is substituted in both cases.

GAC data has a nominal spatial resolution of 4 km where every third scan line and an average of 4 out of every 5 pixels along each scan are used. Fourteen orbits of data collected on 16 March 1994 from the NOAA-14 spacecraft were processed. The delivery includes the orbit data files, output 32 bit files as described in the cloud mask ATBD and output visualization files which allow the user to trace the cloud mask processing path and visualize test results in the satellite projection. As with the previous test data set deliveries, both the orbit data files and the output visualization files can be displayed by the MERLIN software package, which is freeware available from the SDST. Figure 1 is an example of a partial GAC orbit from 16 March 1995

covering the region from the North Pole all the way south across Antarctica. Instrument observations, processing path, a sample of the individual test results and the final cloud mask confidence level product are shown. Comments and suggestions on the test data sets are encouraged.

Cloud Mask Spectral Test Confidences

In the cloud mask algorithm, the result of each spectral threshold test is expressed as a "confidence" which indicates the strength of the observed radiance signature compared to that which is expected for an obstructed field of view. An effort has been made to define a confidence-setting algorithm which may be used for all tests. For example, the "cold cloud test" over open waters requires that any scene with an observed 11 micron brightness temperature colder than a threshold of about 270°K must be at least partially cloudy. The actual cutoff temperature for any given FOV varies slightly because of differing amounts of atmospheric water vapor attenuation due to changes in water vapor content or instrument viewing angle. Consequently, a "confidence window" is constructed with boundaries at 267° and 273°K. Conforming to the ultimate goal of the algorithm, which is to specify a confidence of clear sky, an observed brightness temperature < 267°K is defined to have 0% confidence while a measurement of > 273°K has 100% confidence; observations between 267° and 273°K have confidences that range linearly between 0 and 100%.. In the cold cloud test, the confidence refers to the probability that the FOV did not contain opaque, cold clouds. Figure 2 shows the relationships between test thresholds, confidence boundaries, and observations. Note that the threshold value corresponds to a confidence of 50%. All spectral test confidences are defined in an analogous fashion.

Further effort was made to define the shape and slope of "confidence functions" (the sloping line in the figure). Within confidence windows, varying degrees of non-linearity were applied. For example, one can construct a function which increases slowly at either end of the window but more quickly near the threshold, or conversely, one that increases rapidly near the endpoints and slowly near the center. The "anchor point", or the position of the 50% confidence/threshold value may also be adjusted, leading to asymmetric functions. It was discovered that these changes made little or no difference in the outcome of the final confidence of clear sky for the vast majority of cases.

Generation of Clear Sky Radiance Maps

Work has begun on the design and implementation of clear sky radiance data maps for use in the cloud mask algorithm. A prototype map has been created for the AVHRR Local Area Coverage (LAC) cloud mask which has a spatial resolution of 5 km and extends from 20°-60° North Latitude and 65°-125° West Longitude. Using archived data from May 8-18, 1989, the cloud mask program wrote daytime clear-sky information to a binary file. The stored values for each 5 km grid box were: number of clear-sky observations, sum of 11 micron brightness temperatures, minimum and

maximum 11 micron brightness temperatures. Due to orbital precession of the NOAA-11 spacecraft, the period was broken into 3 time sections. This allowed for close inspection of two separate regions of the upper midwest at near-nadir view angles as well as for comparison of one region at both beginning and ending time periods.

No attempt has been made to implement previously recorded clear-sky data into cloud mask production, but it is obvious that the procedure will need to be accomplished with great care. The maps demonstrated the expected temporal variability due to synoptic-scale weather changes, but also showed surprisingly large spatial differences over fairly small distances, and these in regions usually thought of as being somewhat homogeneous.

Cloud Mask Meeting

The MODIS Cloud Mask Team met in Madison, Wisconsin on 18-19 October to discuss the MODIS cloud masking algorithms. Several conclusions and action items resulted.

A subset follows:

(1) The combination of test confidences has been changed. The new version groups spectral tests by the cloud type most readily detected. A group confidence result is determined, which is the minimum confidence from among the spectral tests within the group. The final FOV confidence is the product of all the group confidences. This procedure reduces the occurrence of low FOV confidence caused by multiplying many moderate to high individual test confidences. Tests which are sensitive to the same cloud type should produce similar confidences.

(2) It was agreed that a simple normalized difference snow index (NDSI) will be implemented in the cloud mask software as a quick check for snow backgrounds. This will account for recent snowfall or melt. George Riggs, a snow mask group representative, suggested a conservative NDSI threshold for testing.

(3) In response to both users' requests and UW quality analysis needs, the 32 bit cloud mask product output file structure has been increased to 48 bits. The new file structure includes bit information on all individual tests, instead of groups of tests, and also includes a non-cloud obstruction (NCO) bit and spares in case others are added in the future. To trace the source of cloud mask errors, pixel level information for each test can now be examined. The increase in file size has been approved by the atmosphere group liaison, Rich Hucek. The new file structure is defined in Table 1.

MODIS Infrared Calibration

The MODIS Thermal Infrared Calibration Algorithm was reviewed in Madison, Wisconsin on 8 - 9 November. MCST presented the algorithm and quality assurance

plans. UW found that the infrared calibration algorithm has matured considerably over the last twelve months. The overall reaction to the ATBD was positive; the IR calibration algorithm has flexibility for adjustment to inflight conditions. The MCST was commended for the quality of this effort. Several comments and actions are summarized briefly below

(1) UW intends to conduct a detailed analysis of the infrared calibration algorithm. MCST will make sure that boundary conditions (e.g. unit reflectance of mirror, small alpha robustness,...) meet expectations in the final expression.

(2) UW display tools for investigating the vacuum test data on site were presented. They enable quick review of large amounts of Thermal Vacuum Calibration test data so that one level of testing can be determined to have been successfully completed before progressing to the next level. MCST will consider use at the Flight Model tests.

(3) UW recommended that the upcoming vacuum tests should characterize non-linearity at cold detector temperatures for all instrument temperatures (lo, mid, hi) and at nominal instrument temperatures for all detector temperatures (cold, mid, hi). This emphasizes early in flight performance and the possibility of floating detector temperatures.

(4) The Test Analysis Computer (TAC) system procedure for calculating system responsivity, space view offsets, and detector nonlinearity are being reviewed by UW. This is in response to larger than expected nonlinearity for low signal levels on some of the photovoltaic (PV) bands in the Engineering Model blackbody cool down test data.

(5) The possible role of the solar diffuser as a second blackbody will be explored by MCST. The question remains whether the temperature with the door open is substantially cooler than the instrument.

GOES Fire and Smoke/Aerosol Detection

In separately funded work, the GOES Automated Biomass Burning Algorithm (to locate and provide estimates of sub-pixel fire size) has been modified to enable monitoring throughout South America. Modifications include an expanded surface vegetation classification scheme (based on the World Ecosystems Map, Olson, 1989-1991) and associated 4 and 11 μm emissivity factors. In addition, NMC model estimates of total precipitable water (2.5° by 2.5°) have been incorporated into the algorithm to account for water vapor attenuation in the 4 and 11 μm bands. Recently, the GOES-8 ABBA also incorporates visible data in an effort to screen sub-pixel cumulus cloud contamination for background temperature calculations in the 4 and 11 μm bands. An initial version of the algorithm provided diurnal (3-hourly) estimates of fire activity during the SCAR-B field experiment.

An automated GOES multispectral aerosol detection algorithm is near completion and will enable more quantitative analyses of the extent and transport of smoke/aerosols observed in GOES satellite imagery (Prins and Menzel, 1995a). GOES visible and infrared (4, 11, and 12 μm) data have been incorporated into a multispectral thresholding scheme. The visible band is used to isolate pixels with brightness counts indicative of haze. Single band thresholds in the 4, 11, and 12 μm bands as well as the 4 minus 11 μm difference and the 11 minus 12 μm difference are used to screen for opaque clouds, semi-transparent cirrus, stratus, and low-level moisture. Data collected from 24-29 August 1988 were used to develop and test a preliminary version of the algorithm. During this time period there was a smoke/aerosol episode that consisted of large-scale aerosol transport and multi-level cloud activity, including semi-transparent cirrus and low-level stratus. Additional work is needed to distinguish aerosols from isolated cumulus activity and in identifying smoke in the vicinity of thin cirrus and along gradients between clear and cloud contaminated pixels. Furthermore, solar zenith angle considerations must be included to distinguish aerosols from sun glint.

During the SCAR-B field program, UW provided the mission scientists in Brazil with GOES-8 satellite imagery, GOES ABBA fire products, meteorological observations, and NMC model output via the UW-Madison SSEC SCAR-B web site (Bywaters and Prins, 1995). The web site consisted of three components: GOES-8 imagery loops (3-hourly visible and infrared), GOES-8 ABBA products, and the McWEB forecasting tool. This interactive tool allowed the scientists to access meteorological information as well as satellite imagery and satellite derived fire products from the Mission Operations Center at IBAMA. The web page provided daily plots of fire locations at peak burning times (11:45, 14:45, 17:45, and 20:45 UTC) for the region extending from approximately 40 to 70°W and from the equator to 30°S. A text summary of daily peak fire statistics from the GOES-8 ABBA was also available. The page contained a morning (11:45 UTC) and afternoon (17:45 UTC) GOES-8 visible image with outlines depicting the areal extent of smoke/aerosol coverage based on an analysis of visible and infrared imagery.

Preliminary GOES-8 ABBA results obtained during SCAR-B (15 August-15 September 1995) suggest that the peak burning time is in the middle of the afternoon (1745 UTC). The number of fires detected at 1745 UTC is 2 to 4 times greater than that observed 3 hours earlier or later and 20 times greater than that observed at 1145 UTC (Prins and Menzel, 1995c). Although the burning pattern is similar to that observed with the GOES-7 ABBA in 1988, the improved spatial resolution available with GOES-8 provides much greater detail concerning fire activity and other surface features (Menzel and Prins, 1995). As in previous years, large smoke palls were identified in the GOES-8 visible imagery. During SCAR-B smoke was evident over a large portion of the continent east of the Andes Mountains. A large smoke pall

covering over 4 million km² was observed from 21 August through 11 September 1995. At the height of the burning period the smoke pall extended over nearly 7 million km². Transport over the Atlantic Ocean was observed on 13 days during the SCAR-B field program. On at least two days, a thin plume of smoke was tracked to the Prime Meridian. The burning practices and meteorological conditions which contributed to this episode are nearly identical to ones which resulted in a similar smoke pall observed during the last week of August 1988 (Prins and Menzel, 1995c).

MAS SCAR-B fire scene calibration

Absolute calibration of MAS SCAR-B hot (fire) scenes is under investigation. Hot scene calibration is difficult because scene temperatures are far above the temperature setting of the MAS warm blackbody calibration source. A laboratory data set viewing a controlled external hot source (up to 500°C) was collected by ARC personnel in October 1995. The data set however suffered from a focusing problem on the external hot source. Using radiative transfer, the filling fraction of the external hot source in the MAS IFOV has been estimated and is being applied to adjust the radiance of the external source as viewed by the MAS. The adjusted external source radiances have been plotted against MAS 1.6 and 2.1 micron observations and show a linear relationship with both channels. Because of the focus problem, the hottest effective external source radiances observed by MAS were less than 400°C; scenes hotter than 400°C will require significant extrapolation of the MAS count to radiance relationship. Information on the effective emissivity of the external hot source is still required to account for spectral emissivity variation of the external hot source.

Split Window Cloud Studies

MAS, GOES-8, HIS, and AVHRR data are being used in an investigation of negative 11 micron minus 12 micron (T11-T12) occurrences. MAS and HIS comparisons (January 1995 data set) suggest that MAS T11-T12 differences are biased negative. MAS blackbody emissivity corrections reduce the magnitude, however MAS T11-T12 remains negatively biased compared to HIS T11-T12. GOES-8 and AVHRR T11-T12 also exhibit negative differences. These show temporal and spatial consistency in scenes of vigorous convective growth, lending credibility to the hypothesis that negative differences are related to cloud microphysics. Modeling microphysical properties is needed to support the GOES and AVHRR observations. Observations by MAS and HIS of vigorous convective growth are needed to corroborate the satellite observations. A poster on this topic will be presented in January at the 8th Conference on Satellite Meteorology and Oceanography

DATA ANALYSIS

MAS 50 Channel Cloud Mask

In preparation for the MODIS day-1 cloud mask product, data from the 50 channel MODIS Airborne Simulator (MAS) is being used to develop a multispectral cloud mask algorithm. The spectral tests used to determine an unobstructed confidence level rely on radiance (temperature) thresholds in the infrared and reflectance thresholds in the visible. These thresholds vary with surface type, atmospheric conditions (moisture, aerosol, etc.) and viewing geometry. A necessary part of the algorithm development is to characterize the individual spectral test thresholds as a function of these variables.

Confidence flags convey strength of conviction in the outcome of the cloud mask algorithm tests for a given FOV. When performing spectral tests, as one approaches a threshold limit, the certainty or confidence in the outcome is reduced. Therefore, a confidence flag for each individual test, based upon proximity to the threshold value, is assigned and used to work towards a final quality flag determination for the FOV outcome. The current scheme applies a linear interpolation between a low confidence clear threshold (0 % clear confidence) and high confidence clear threshold (100 % clear confidence) for each spectral test. The initial FOV determination is a combination of the confidences of all applied tests (as described earlier). This determination will dictate whether additional testing (using spatial variability tests) is warranted to improve the confidence. The final quality flag determination will be clear or cloudy with a confidence level associated with it. This approach is being considered as a method of quantifying our confidence in the derived cloud mask for a given pixel.

The relatively small geographical coverage of MAS data sets make it difficult to study global spectral threshold regimes; however, with global observations provided by the coarser spectral and spatial resolution AVHRR/HIRS data sets, a cloud mask algorithm can be determined which takes advantage of the strengths of each instrument. For example, an unobstructed CO₂ channel (13.9 micron) threshold of 245 K was set by examining global clear sky HIRS observations as determined from Collocated HIRS/2 and AVHRR ProductS (CHAPS) processing.

Combining the strengths of both the global and regional data sets, a MAS 50 channel cloud mask algorithm has been developed. Both a tropical ocean scene (Gulf of Mexico, 13 January 1995) and a polar land scene (Alaska, 21 April 1995) were chosen to test the algorithm. Observations and key results are depicted in Figure 3. The two flight segments were chosen to test the cloud mask in extremes of surface and atmospheric conditions.

The top panels of Figure 3 were collected during the 21 April 1995 MAS ER-2 flight over Alaska along the 65th parallel. In this case, north is to the right. The reduced resolution swatches have an areal extent of approximately 40 x 120 km. Very thin cirrus overlays the entire flight track. This is not obvious from the .66 micron image (top left panel), where surface features can be readily identified, nor from the 11 micron image (top, 3rd panel from left), where only a few cloud filaments provide enough thermal contrast with the background to be identified. Infrared temperatures over most of the scene range between 264 and 268 K. The cloud mask algorithm utilizes a 1.88 micron channel reflectance threshold test, which has similar spectral characteristics to the 1.38 micron MODIS channel, for the detection of thin cirrus. The strong water vapor absorption in the 1.88 micron region masks the surface reflectance whereas high clouds are unobscured. This allows even thin cirrus to be easily identified (Figure 3, top, second from the left). For this entire flight segment, the 1.88 micron reflectance value exceeded the low cloud confidence clear threshold

cutoff (.20%) (Figure 3, top, 5th panel from the left). This results in the entire flight track being labeled as clear confidence less than 1%.

As described earlier, the snow mask and cloud mask groups have agreed that a preliminary version of the snow mask algorithm will be included as part of the cloud mask production software. This will be used to identify cloud mask background algorithm processing paths. Snow is flagged if the NDSI,

$$NDSI = \frac{(r_{.55micron} - r_{1.62micron})}{(r_{.55micron} + r_{1.62micron})},$$

is greater than .40, and if the .87 micron reflectance is greater than 10%. Here $r_{.55}$ and $r_{1.62}$ refer to the reflectance at .55 and 1.62 microns respectively. Figure 3, top, 4th panel from the left depicts the algorithm processing path for the 21 April 1995 flight. Dark areas are regions where the polar land cloud mask algorithm was run; light gray regions show where the snow cloud mask algorithm is implemented (NDSI found snow).

The far right top panel of figure 3 demonstrates the utility of defining a snow background processing path. The panel depicts the results of applying the APOLLO thin cirrus test

$$T_{11micron} - T_{12micron} > Thresh(T_{11micron}, \Psi),$$

to the scene. The dynamic threshold is a function of the viewing zenith angle Ψ and the 11 micron brightness temperature, which represents the amount of water vapor attenuation. Snow and ice backgrounds can mistakenly be identified as cloud by this test; therefore, the APOLLO test was only applied to scenes which were not flagged as snow by the NDSI (light gray region). The black region is where the test was applied but no cloud was found, and the white region represents portions of the scene where the test was applied and cloud was detected. Although this test did not detect all cirrus in the scene, it will assist in identifying cirrus cloud when the 1.88 micron reflectance test is not available (i.e., night).

The bottom 6 panels of Figure 3 are images from the 13 January 1995 MAS overflight of the Gulf of Mexico. Both optically thin and thick cirrus (top of images) along with small cumulus clouds (bottom portion of images) were observed. The flight segment was processed using the MAS 50 channel cloud mask algorithm. MAS observations and most relevant tests are depicted. The first three panels on the bottom of Figure 3 are spectral observations at .66, 1.88, and 11 microns. Note how only the high cloud is observed in the 1.88 micron channel image, whereas the cumulus clouds are best defined in .66 micron image. The visible reflectance ratio test ($r_{.87}$ micron/ $r_{.66}$ micron) flags primarily the cumulus cloud (Figure 3, bottom, 4th from the left) whereas the high cloud is detected by the 1.88 micron reflectance threshold test (Figure 3, bottom, 5th from the left). The strengths of these tests are combined to

produce the resultant cloud mask (Figure 3, bottom, last panel), defining the final clear confidence. Decreasing confidence coincides with lighter gray shades. Low confidence clear (< 1%) results are shaded white. These areas match up very well with the observed clouds. The regions of lower confidence clear (<66 and < 95%) observed along the left and right edges of the cloud mask image are a result of the longer atmospheric path length, which increase the Mie and Rayleigh scattering components, causing the visible reflectance values to exceed the threshold. This effect must be compensated for in the final MODIS cloud mask through scan angle dependent thresholds.

Comparison of ATSR SST to Surface Measurements

Data acquired during the OTIS (Ocean Temperature Interferometer Sensing) experiment in the Gulf of Mexico in January 1995 were analyzed by Liam Gumley to determine the agreement between ATSR SST and surface (R/V Pelican) measurements of SST. ATSR 1-km resolution data was provided by Ian Barton at CSIRO. An ATSR scene from January 16 was used in the analysis. The ATSR overpass was at 1713 UTC, while the Pelican traversed the region covered by the ATSR pass between 0130 and 0800 UTC. A simple cloud mask based on reflectance, window brightness temperature, and 11-12 micron brightness temperature thresholds was used for cloud screening. Once the clear pixels in the ATSR scene were identified, the ship track was overlaid on the ATSR scene to determine collocation. Fifteen collocation points were found; however 5 of these points were either cloud covered in the ATSR image, or at the edge of clouds. The ATSR data showed excellent agreement with surface measurements of SST derived from the AERI instrument. The RMS bias between ATSR and AERI was 0.02 K, while the RMS bias between ATSR and the R/V Pelican surface skimmer SST was 0.16 K. Further analysis of these data will be done as part of a demonstration of capability for in-orbit validation of the MODIS IR bands.

MAS Infrared Calibration

Characterizing MAS calibration continues. During summer 1995, spectral response measurements for all 50 MAS channels were made at the Ames Research Center (ARC) calibration facility. A one quarter meter single grating monochromator with a light source consisting of a 100 watt tungsten halogen lamp and a 100 watt Nernst glow bar were used for the measurements. The MAS output and calibrated reference detector signals were recorded at the grating monochromator step rate. Dan LaPorte and Chris Moeller participated in the experiment design and measurements at ARC in July. A finalized set of measurements were produced at ARC in August. The spectral response measurements were post-processed at the UW. Processed spectral response data for all 50 MAS spectral bands were delivered to NASA GSFC in the fourth quarter of 1995. The raw spectral response data were corrected for the background (reference) spectrum, and for atmospheric absorption along the measurement optical path using guidance from FASCOD3. A smoothing Savitsky-Golay smoothing filter which preserves bandpass halfwidth was applied and the data were normalized to the

maximum response in each band. The normalized SRF data for MAS thermal channels (Figure 4) are much improved over the Stennis Space Center SRF data set (8/94). Noise in the SRF curves is much reduced and spectral features due to atmospheric attenuation are effectively removed from the curves. A set of spectral response measurements was also made in October 1995 at the ARC calibration facility using Fourier Transform Infrared (FTIR) technology. Dan LaPorte participated in the experiment setup and data collection at ARC. FTIR technology has the benefit of completely filling the MAS aperture and IFOV, reducing subpixel filling effects and improving signal to noise in the measurements. The FTIR measurements are very good, showing accurate spectral registration and many high spectral resolution atmospheric attenuation features. These FTIR measurements are being post-processed at UW and are being compared to grating system measurements also made in October 1995.

MAS calibration blackbody emissivity has been estimated for all infrared channels. A laboratory data set of MAS viewing the well calibrated Advanced Kinetics Extended Area Blackbody Source was used for this work. Previously, an assumption of unit emissivity was used for all MAS infrared calibration. However, comparisons with High-resolution Interferometric Sounder (HIS) data have indicated that this assumption caused systematic error in the MAS absolute calibration for earth-atmosphere scene temperatures. MAS effective emissivity is estimated to be around 0.98 for SWIR channels (26-41) and around 0.94 for LWIR channels; however, strong CO₂ absorption causes elevated effective emissivity estimates for CO₂ sensitive channels. These require further analysis to remove all intervening atmospheric attenuation effects from the data set. Estimated emissivities for MAS window channels along with the brightness temperature correction for typical ocean and cloud scene temperatures are shown in Table 2. The correction is a function of both emissivity and MAS instrument temperature. MAS spectrometer head temperature (typically 0 to -10°C) is monitored inflight and is currently being used to characterize the MAS instrument temperature. Laboratory measurements of MAS blackbody reflectivity are planned for the next quarter. Those measurements will be compared to the emissivity estimates listed in Table 2.

The normalized SRF data and emissivity estimates are being incorporated into MAS infrared absolute calibration. New comparisons between MAS and the High-resolution Interferometric Sounder (HIS) data have been made using clear Gulf of Mexico scene data collected in January 1995. The LWIR MAS-HIS comparisons are shown in Figure 5. In accounting for non-unit emissivity, MAS-HIS biases change from positive to negative for most of the longwave infrared channels. Channels 48-50 still show aberrant behavior which is attributed to the effects of atmospheric attenuation in the laboratory data set. A remaining fairly consistent bias in channels 42-47 may be due to error in the representation of the MAS instrument temperature. Future thermal vacuum chamber laboratory measurements and additional inflight monitoring will reduce MAS instrument temperature uncertainty.

PAPERS

Ackerman, S. A., K. I. Strabala, R. A. Frey, C. C. Moeller and W. P. Menzel, 1995: Cloud Mask for the MODIS Airborne Simulator (MAS): Preparation for MODIS. Presented at the AGU Fall Meeting, Science and the First EOS Platform, EOS-AM1 session held in December and accepted as a poster for the 76th AMS Conference, Atlanta, GA. Jan. 28-Feb. 2, 1996, pp (TBD).

Ackerman, S. A., 1995. Global satellite observations of negative brightness temperature differences between 11 and 6.7 microns. Accepted with revisions to *J. of Atmos. Science*.

Bywaters, K.W., and E.M. Prins, 1995: An interactive WWW tool for coupling satellite and meteorological data in real time. Accepted as a paper for the 76th AMS Conference, Atlanta, GA. Jan. 28-Feb. 2, 1996, pp (TBD).

Gumley, L.E., and M.D. King, 1995: Remote Sensing of Flooding in the U.S. Upper Midwest during the Summer of 1993. *Bull. Am. Met. Soc.*, **76**, 933-943.

Gumley, L.E., Van Delst, P., Moeller, C., and W.P. Menzel, 1995: Satellite and airborne IR sensor validation by an airborne interferometer. Accepted for the 2nd International Airborne Remote Sensing Conference, June 24-27 1996, San Francisco CA.

King, M. D., W. P. Menzel, P. S. Grant, J. S. Myers, G. T. Arnold, S. Platnick, L. E. Gumley, S. Tsay, C. C. Moeller, M. Fitzgerald, K. S. Brown, and F. Osterwisch, 1995: Airborne scanning spectrometer for remote sensing of cloud, aerosol, water vapor and surface properties. Submitted to *Jour. Atmos. and Oceanic Tech.*

Menzel, W.P., and E.M. Prins, 1995: Monitoring biomass burning with the new generation of geostationary satellites. Accepted for publication in the Proceedings of the AGU Chapman Conference on Biomass Burning and Global Change, Williamsburg, VA, March 13-17, 1995, J.S. Levine (Ed.), Cambridge MA, The MIT Press.

Moeller, C.C., S. A. Ackerman, K. I. Strabala, W. P. Menzel and W. L Smith, 1995: Negative 11 micron minus 12 micron brightness temperature differences: A second look. Accepted as a poster for the 76th AMS Conference, Atlanta, GA. Jan. 28-Feb. 2, 1996, pp (TBD).

Prins, E.M., 1995: Biomass Burning, in *Encyclopedia of Environmental Biology: Volume 1*, edited by W. A. Nierenberg, pp. 309-325, Academic Press, San Diego, CA.

Prins, E.M., and W.P. Menzel, 1995a: Investigation of biomass burning and aerosol loading and transport utilizing geostationary satellite data. Accepted for publication in

the Proceedings of the AGU Chapman Conference on Biomass Burning and Global Change, Williamsburg, VA, March 13-17, 1995, J.S. Levine (Ed.), Cambridge MA, The MIT Press.

Prins, E.M., and W.P. Menzel, 1995b: Monitoring fire activity in the western hemisphere with the new generation of geostationary satellites. Accepted as a paper to be presented at the 22nd Conference on Agricultural and Forest Meteorology with Symposium on Fire and Forest Meteorology, Atlanta, GA, Jan.28 - Feb.2, 1996, pp (TBD).

Prins, E.M., and W.P. Menzel, 1995c: Monitoring biomass burning and aerosol loading and transport from a geostationary satellite perspective. Accepted as a paper to be presented at the Seventh Symposium on Global Change Studies, Atlanta, GA, Jan.28 - Feb.2, 1996, pp (TBD).

Smith, W. L., R. O. Knuteson, H. E. Revercomb, W. Feltz, H. B. Howell, W. P. Menzel, N. Nalli, O. Brown, J. Brown, P. Minnett, and W. McKeown, 1995: Observations of the infrared radiative properties of the ocean - Implications for the measurement of sea surface temperature via satellite remote sensing. Accepted by Bull. Amer. Meteor. Soc.

MEETINGS

Chris Moeller and Dan LaPorte participated in the MAS spectral response measurements performed at Ames Research Center on 10-13 July.

Paul Menzel attended the review of SDST and MCST at GSFC on 17-18 July.

Dan LaPorte attended the Calibration Workshop held in Wallops Island, VA the week of 7 August .

Steve Ackerman attended the SASS meeting held at Ames Research Center on 29-31 August.

Dan LaPorte attended the Calibration Peer Review held at Santa Barbara, CA on 13-14 September.

Steve Ackerman attended the snow and ice workshop held at GSFC on 13-14 September.

Dan LaPorte attended the MCST Calibration review on 20-21 September.

Elaine Prins attended the IGBP-DIS Global Fire Monitoring Workshop at the European Joint Research Centre in Ispra, Italy on 17-19 October, 1995 and gave presentations on "Monitoring Diurnal Fire Activity and Aerosol Transport in the

Western Hemisphere with GOES-8” and “An Overview of the SCAR-B Field Program” and chaired a discussion group on “Research and Development Plans and Priorities”.

The UW hosted a cloud mask meeting in Madison 18-19 October.

Kathy Strabala attended the Science Advisory Panel meeting at GSFC 24-25 October.

Dan LaPorte participated in FTIR based MAS spectral response measurements 30-31 October.

Paul Menzel attended the Aerosol Interdisciplinary Program Workshop held at the Columbia Inn in Columbia, MD on 30 October - 1 November 1995 and gave a presentation on the “Investigation of Biomass Burning and Aerosol Loading and Transport in South America Utilizing Geostationary Satellites”.

The UW hosted a review of the MCST at Madison 8-9 November.

Dan LaPorte assisted in the review of the EM black body cool down at GSFC on the TAC system on 13 November.

Liam Gumley and Kathy Strabala attended the MODIS programmers forum at NASA GSFC on 14 November.

Paul Menzel, Steve Ackerman, Liam Gumley, Chris Moeller, Dan LaPorte and Kathy Strabala attended the MODIS Science Interest Group Meeting at NASA GSFC on 15-17 November 1995. Moeller presented materials on MAS infrared calibration to the Atmosphere’s Group on 14 November.

Steve Ackerman presented a paper on the development of the MODIS cloud mask at the AGU Fall Meeting, Science and the First EOS Platform, EOS-AM1 session held in December in San Francisco.

Table 1. Updated MODIS Cloud Mask 48 Bit Structure

Bit Group	Number of bits	Bit Value Description
Decision	1	1 mask determined, 0 no decision
Summary of all algorithms	2	unobstructed FOV (quality flag) 11 > 99% prob of clear 10 > 95% prob of clear 01 > 66% prob of clear 00 cloud
Processing path	1	day or night processing (1 day, 0 night)
	1	sun glint regime (1 no, 0 yes)
	1	snow/ice background (1 no, 0 yes)
	2	land/water background (11 land, 10 wetland, 01 coastal, 00 water)
Additional Information	1	Non-cloud obstruction (1 no, 0 yes)
	1	Thin cirrus detected (1 no, 0 yes)
	1	Shadow found (1 no, 0 yes)
Spares	2	
Results from cloud algorithms	1	IR threshold test did not find cloud
cloud (bit set if no cloud found)	1	CO2 high cloud test did not find high cloud
	1	6.7 micron test did not find high cloud
	1	1.88 micron test did not find high cloud
	1	3.7 - 12 micron test did not find high cloud
	1	Tri-spectral BTDIF tests did not find cloud
	1	3.7 - 11 micron test did not find cloud
	1	Visible reflectance test did not find cloud
	1	Reflectance ratio test did not find cloud
	1	.935/.87 reflectance test did not find cloud
	1	3.7-4.0 micron BT test did not find cloud
Additional tests	1	passed temporal consistency test
	1	passed spatial consistency test
Spares	6	
250 m mask from visible tests	16	1 clear, 0 cloud for 16 FOVs in 1 km FOV

TABLE 2. MAS blackbody emissivity and emissivity correction impact.

MAS channel	Central wavelength (μm)	Estimated blackbody emissivity	Ocean scene			
			Ocean scene uncorrected temperature (K)	Ocean scene emissivity corrected temperature (K)	Cloud scene uncorrected temperature (K)	Cloud scene emissivity corrected temperature
31	3.74	0.978	293.2	292.9	257.1	257.5
32	3.90	0.980	291.6	291.3	241.2	242.5
42	8.59	0.942	291.9	290.8	211.7	218.3
45	11.01	0.939	294.1	292.8	213.8	219.2
46	11.97	0.937	293.4	292.0	214.5	219.7

Global AVHRR GAC Cloud Mask Example

Orbit 07:57 UTC

16 March 1995

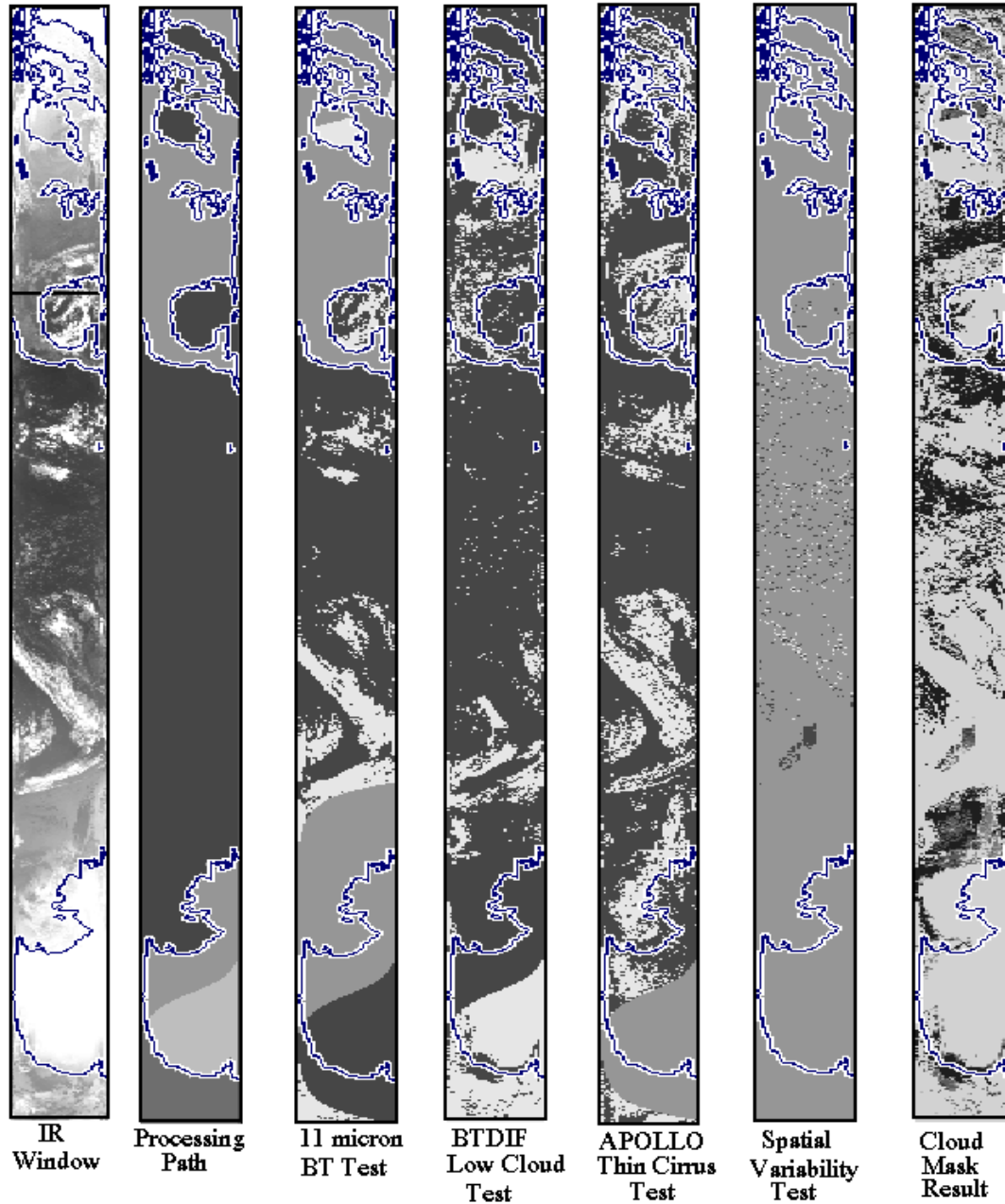


Figure 1. Partial AVHRR GAC orbit depicting 11 micron observations (left image), cloud mask processing path (second image to the left), individual cloud mask test results (middle 4 images) and resultant cloud mask (right image). Different threshold regimes are outlined by the processing path image; for instance, the darkest region indicates that the nighttime ocean algorithm was used, whereas the lightest regions represent the daytime land regime. The individual test results are color coded gray (test not applied), white (test failed - lower confidence clear) and black (test passed - higher confidence clear). The cloud mask result, which is a combination of the individual tests, is shaded light to dark representing low to high confidence clear.

Cloud Mask Test Confidence Determination
Cold Cloud Test Example

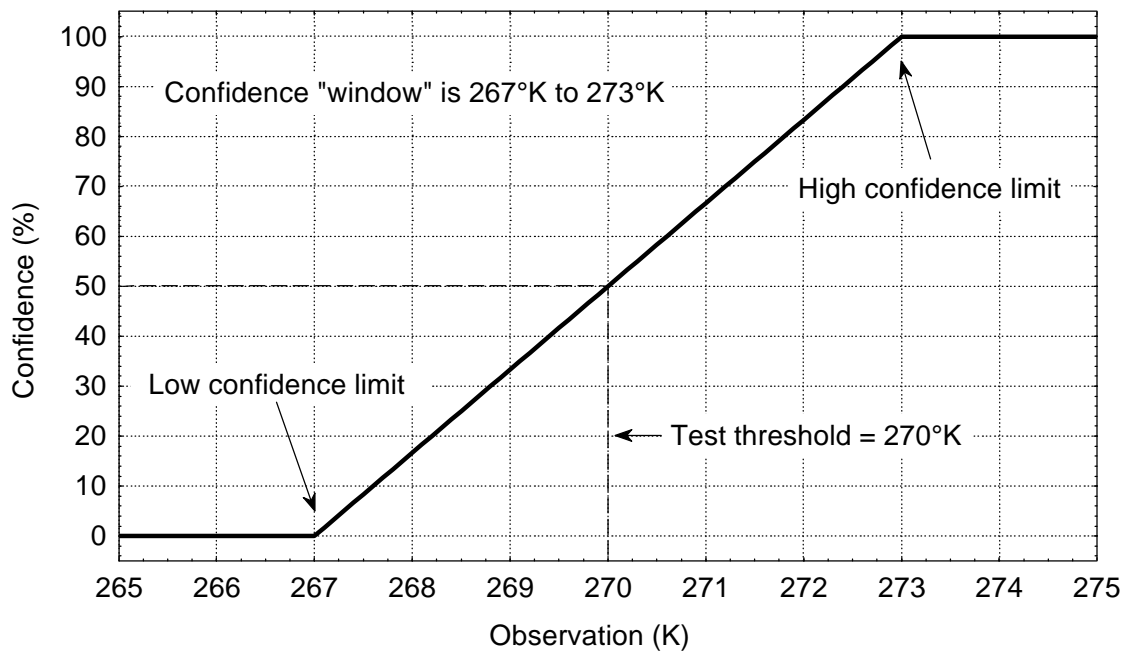


Figure 2. Example test confidence determination showing the relationships between test threshold, confidence boundaries, and observation.

represents the final clear confidence levels of >99% (black), >95% (dark gray), >66% (light gray) and <1% (white).

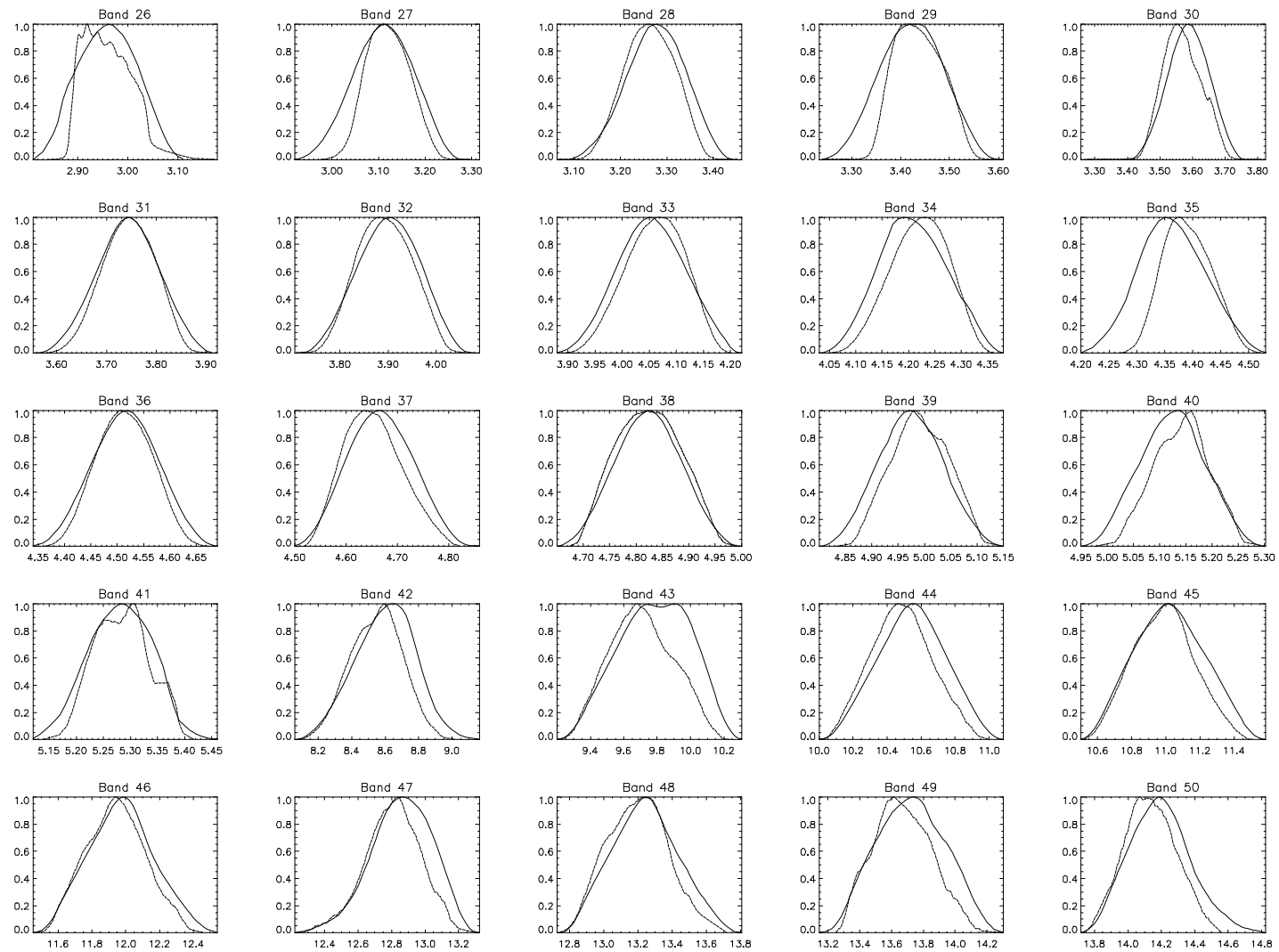


Figure 4. MAS infrared normalized spectral responses from Ames Research Center August 1995 measurements (solid) and Stennis Space Center August 1994 measurements (dashed).

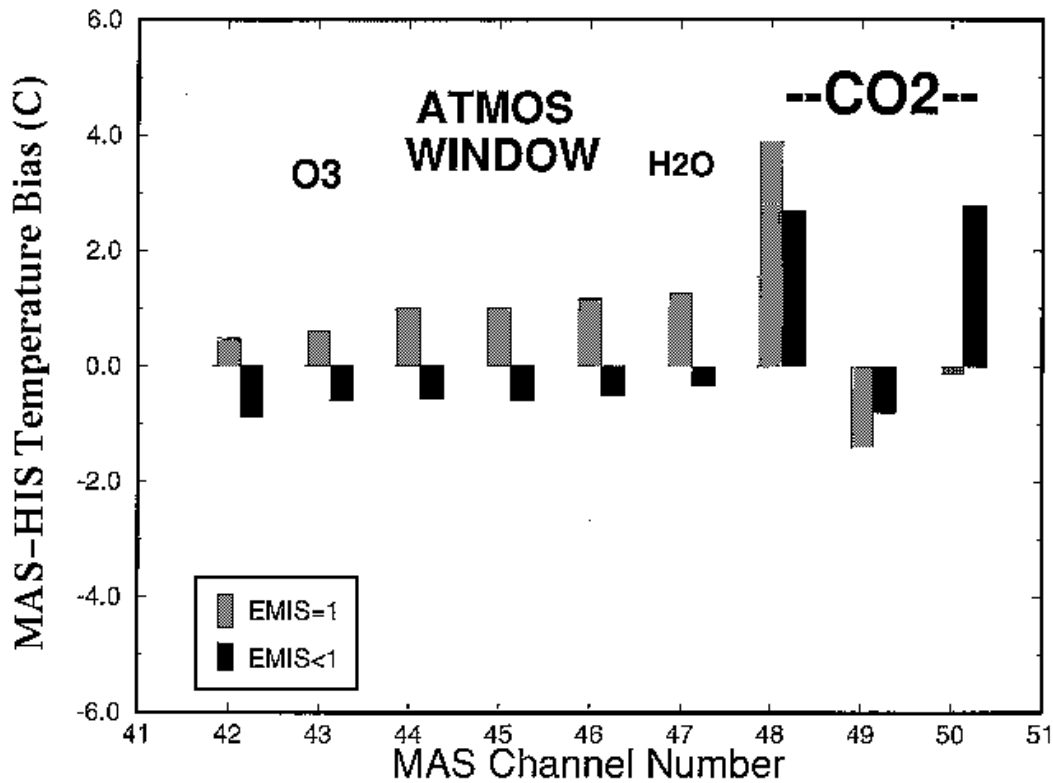


Figure 5. Comparison of the LWIR brightness temperatures between MAS and HIS instruments using clear Gulf of Mexico scene data collected in January 1995. MAS-HIS biases change from positive to negative for most channels when non-unit blackbody emissivity is taken into account.